Proceedings on Automation in Medical Engineering
Proc AUTOMED, 2026, Vol. 3, No 1, Article ID 2495, 2 Pages

Infinite Science Publishing

A cubic model for vessel lumen reconstruction from segmental balloon strain data

B. Agahi[1*], A. Bhave[1,2], K. Möller[1,2]

[1] *The Institute of Technical Medicine, Furtwangen University, Villingen-Schwenningen, Germany*
[2] *Faculty of Engineering, Freiburg University, Freiburg, Germany*
[*] *Corresponding author, email: bag42102@stud.hs-furtwangen.de*

Abstract: Balloon catheters with distributed strain sensors aim to estimate arterial wall mechanics in vivo. Reconstructing the lumen contour from circumferential segment lengths is essential. The standard linear one-parameter mapping proves insufficient for soft-tissue and concave geometries. A smooth cubic model with soft geometric penalties and robust evolutionary optimization achieves accurate closure and area agreement while yielding physiologically realistic curvature.

I. Introduction

Highly compliant elastomer balloons with circumferential strain sensors are being developed to assess arterial wall mechanics in vivo [1]. During controlled inflation, the balloon conforms to the lumen and provides a discrete set of circumferential segment lengths used as input for inverse models estimating healthy and atherosclerotic tissue properties. The previously used linear one-parameter mapping from segment length to local turning angle performs adequately for stiff geometries with mild concavities but fails for soft tissues or deeply concave lumens [2]. To overcome this limitation, a refined mapping is introduced, enabling more accurate and robust lumen reconstruction across both rigid and soft-tissue geometries, including varying concavity depths.

II. Material and methods

The subsections below summarize the data and estimation.

II. I. Reconstruction target and data

A lumen cross-section is reconstructed from the circumferential segment lengths $\{S_i\}_{i=1}^{N}$ measured at a single inflation step; no reference turning angles or landmark coordinates are required. Two scenarios are considered: rigid (no wall compliance, 48 data sets) and soft-tissue (pressure-driven expansion, 5 data sets). All datasets were generated in COMSOL Multiphysics version 6.3, with the balloon discretized into $N = 128$ segments and inflated over 151 pressure steps, as in [2]. Here, an intermediate scale δ_i is defined as

$$\delta_i = \frac{S_i - S_*}{S_*}, \quad S_* \in \{\bar{S}, \tilde{S}\}, \tag{1}$$

where $\bar{S}$ and $\tilde{S}$ denote the mean and median of S_i, respectively. It is introduced to generalize and enable flexible models. After the angles D_i are obtained from the chosen method (Eq. (2) or Eq. (4)) using a suitable optimizer, the lumen contour is generated by forward placement, advancing by S_i and rotating by D_i at each step.

II. II. Linear model

Based on Bhave et al. [2], the cross-section is modeled as a closed N-gon with a linear mapping based on the scale δ_i:

$$D_i = -(k\,\delta_i + \phi_N), \qquad \phi_N = 360°/N\,, \tag{2}$$

where ϕ_N denotes the nominal per-edge turning step. The reconstruction objective combines closure and area errors,

$$Objective \;=\; w_c\, e_{closure} \;+\; w_A\, e_{area}\,. \tag{3}$$

Since $\sum_i \delta_i = 0$ $(for: S_* = \bar{S})$, the total rotation satisfies $\sum_i D_i = -360°$. The gain k is obtained by minimizing the objective in Eq. (3) under the bounds $-180° \le D_i \le 180°$.

II. III. Cubic model

The turning angle is treated as a pointwise functional mapping $D_i = f(\delta_i)$. Plotting the reference turning angle D_i^{ref} against δ_i for the most challenging shapes revealed a consistent cubic trend, with one local maximum, one local minimum, and an inflection point (Fig. 1). Accordingly, it is modeled as a cubic polynomial of the scale δ_i:

$$D_i \;=\; a_3\,\delta_i^3 \;+\; a_2\,\delta_i^2 \;+\; a_1\,\delta_i \;+\; a_0\,. \tag{4}$$

Since the nonlinear mapping does not enforce the full-turn condition $\sum_i D_i = -360°$, a rotation-penalty term is included in the objective (Eq. (5)). The parameters are obtained by minimizing this objective.

$$Objective \;=\; w_c\, e_{closure} \;+\; w_A\, e_{area} \;+\; w_\Sigma\, e_{turn}\,. \tag{5}$$

As the cubic mapping is smooth, the objective remains continuous and avoids search-space fragmentation, enabling Differential Evolution (DE) and Covariance Matrix Adaptation Evolution Strategy (CMA-ES) to explore the parameter space reliably, followed by a short Nelder–Mead (NM) refinement. In addition to the main objective, three geometric constraints are enforced through monotonically increasing, step-wise penalties: (i) a cumulative outward-turn penalty to prevent spiral-like

loops, (ii) a span-deviation penalty to limit unrealistic lateral inflation or shrinkage, and (iii) a per-step turning-range penalty to suppress implausibly large or small angle increments. Each penalty strengthens proportionally to the degree of violation, yielding smooth yet effective regularization that avoids search-space discontinuities and prevents convergence to geometrically invalid shapes.

Because the polygon area—and hence e_{area}— is numerically much larger than the closure error e_{closure}, a dynamic weighting is applied: for larger shapes, the closure weight w_c is scaled up relative to w_A, so that both terms contribute on a comparable scale to the objective.

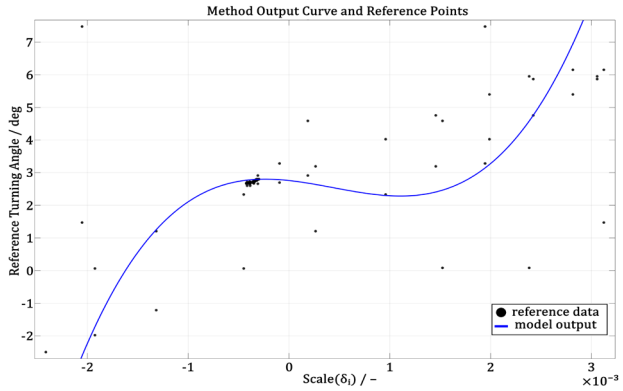

Figure 1: Reference data (dots) vs. cubic model output (line) for scale–angle mapping.

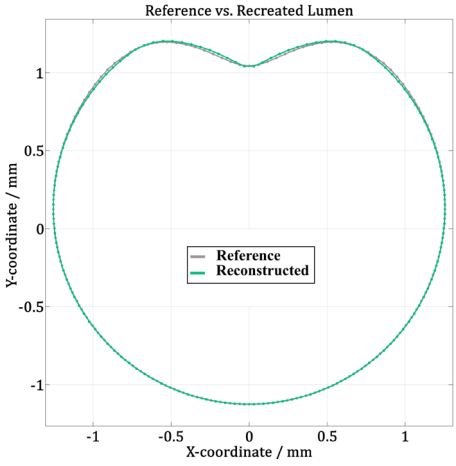

Figure 2: Reference (grey) and reconstructed (green) contour of a soft-tissue case while the baseline method fails to recover it.

III. Results and discussion

Across all soft-tissue cases, the cubic model yielded accurate reconstructions, using CMA-ES followed by a brief NM refinement. Closure error was $<10^{-4}$ mm, area mismatch $<10^{-2}$ mm², span ratios 0.99–1.01, no active span or angle penalties, and convergence occurred in all cases. The best objective (a dimensionless, normalized weighted error) remained below 0.05. Each case required ≈6 s of wall time, with an effective bandwidth of 0.14 GB/s, arithmetic intensity ≈0.25 flop/byte, and per-point–per-evaluation cost $\approx 10^{-7}$ s — indicating a light and stable workload.

Analysis of D_i^{ref} versus δ_i (Fig. 1) shows that each scale value can correspond to multiple, widely differing, turning angles. This intrinsic non-uniqueness prevents any mapping from achieving an ideal fit. Nevertheless, the proposed method absorbs this scatter during parameter estimation and reconstructs contours that closely match the true geometry. Across all datasets, the mean pointwise distance between corresponding original and reconstructed nodes is about 0.031 mm (≈1.25 % of the radius span), while the worst-case deviation remains below 0.043 mm (≈1.7 %). In addition, we quantify a symmetric area error, defined as the total area of regions that are enclosed by exactly one of the two contours (i.e., the summed absolute area of all local under- and over-estimations). This area difference is typically around 0.04 mm², and even in the worst case stays below 0.055 mm² (≈1.2 % of the lumen area).

Beyond the baseline mean-centered δ_i, a median-centered variant is introduced by setting $S_* = \tilde{S}$ in Eq. (1). This shifts healthy segments toward $\delta \approx 0$, causing their turning-angle contribution to be dominated mostly by the constant term (a_0), which often improves the fit. The trade-off is a tighter δ distribution that induces more local minima, thus increasing runtime and requiring stricter optimization (broader global search, more seeds, and restart strategies).

The cubic model is not uniquely identifiable: different parameter sets can produce nearly identical $D(\delta)$ profiles. This non-uniqueness may be intrinsic to the model or a result of the current calibration and search strategy. Future refinements, such as improved identification or a broader δ-range may enforce uniqueness.

Although optical coherence tomography (OCT) and intravascular ultrasound (IVUS) provide accurate lumen geometry [3], they do not capture mechanical properties. The segmented-balloon approach offers lower resolution but reconstructs the lumen adequately (Fig. 2) and provides features for plaque mechanical characterization.

Future work will classify healthy and diseased regions from their geometric evolution across inflation steps, and improve accuracy through multi-stage sequential reconstructions rather than single-step analysis.

IV. Conclusions

Lumen cross-sections can be reconstructed directly from circumferential segment lengths, enabling catheter-based assessment of regional arterial mechanics. The proposed cubic mapping, combined with geometric regularization and evolutionary optimization produced accurate, stable, and lightweight reconstructions across all cases.

Author's Statement

This research was partly supported by the German Federal Ministry of Research and Education (BMBF) Grant number 13FH066KX2 (DiaKatPlus/FH-Kooperativ). Conflict of interest: Authors state no conflict of interest.

References

[1] Bhave, A., Sittkus, B., Urban, G., Mescheder, U. and Moeller, K. Finite element analysis of the interaction between high-compliant balloon catheters and non-cylindrical vessel structures: towards tactile sensing balloon catheters. Biomechanics and Modeling in Mechanobiology, 22, 2023, pp.2033-2061.

[2] Bhave, A., Rupitsch, S.J. and Moeller, K. Simplified inverse model for basic lumen shape identification. Current Directions in Biomedical Engineering, 11(1), 2025, pp.322-325.

[3] Kubo, T., Akasaka, T., Shite, J., Suzuki, T., Uemura, S., Yu, B., Kozuma, K., Kitabata, H., Shinke, T., Habara, M., Saito, Y., Hou, J., Suzuki, N. and Zhang, S. OCT compared with IVUS in a coronary lesion assessment: The OPUS-CLASS study. JACC: Cardiovascular Imaging, 6(10), 2013, pp.1095-1104.